Gene Therapy (2018) 25:524–537
https://doi.org/10.1038/s41434-018-0043-6

ARTICLE

Corrected: Correction

Epistasis between *Pax6*^{Sey} and genetic background reinforces the value of defined hybrid mouse models for therapeutic trials

Jack W. Hickmott[1,2] · Uvini Gunawardane[1] · Kimberly Jensen[1] · Andrea J. Korecki[1] · Elizabeth M. Simpson[1,2,3,4]

Received: 17 May 2018 / Revised: 2 September 2018 / Accepted: 5 September 2018 / Published online: 26 September 2018

Abstract

The small eye (*Sey*) mouse is a model of PAX6-aniridia syndrome (aniridia). Aniridia, a congenital ocular disorder caused by heterozygous loss-of-function mutations in *PAX6*, needs new vision saving therapies. However, high phenotypic variability in *Sey* mice makes development of such therapies challenging. We hypothesize that genetic background is a major source of undesirable variability in *Sey* mice. Here we performed a systematic quantitative examination of anatomical, histological, and molecular phenotypes on the inbred C57BL/6J, hybrid B6129F1, and inbred 129S1/SvImJ backgrounds. The *Sey* allele significantly reduced eye weight, corneal thickness, PAX6 mRNA and protein levels, and elevated blood glucose levels. Surprisingly, *Pax6*$^{Sey/Sey}$ brains had significantly elevated *Pax6* transcripts compared to *Pax6*$^{+/+}$ embryos. Genetic background significantly influenced 12/24 measurements, with inbred strains introducing severe ocular and blood sugar phenotypes not observed in hybrid mice. Additionally, significant interactions (epistasis) between *Pax6* genotype and genetic background were detected in measurements of eye weight, cornea epithelial thickness and cell count, retinal mRNA levels, and blood glucose levels. The number of epistatic interactions was reduced in hybrid mice. In conclusion, severe phenotypes in the unnatural inbred strains reinforce the value of more naturalistic F1 hybrid mice for the development of therapies for aniridia and other disorders.

Introduction

In humans, aniridia is a penetrant monogenic disorder with high phenotypic variability, even between family members with the same mutation [1]. Loss-of-function paired box 6 (*PAX6*) mutations, most frequently premature termination codons (http://lsdb.hgu.mrc.ac.uk/home.php?select_db=PAX6) [2], cause *PAX6*-aniridia syndrome (aniridia, OMIM: 106210). The result of PAX6 haploinsufficiency, aniridia is a rare genetic disorder predominantly affecting the eyes, central nervous system, and pancreas [3–13]. People with aniridia are born with low vision, with diagnosis occurring shortly thereafter when the eponymous iris hypoplasia is readily detectable. In addition to congenital fovea hypoplasia and lens abnormalities that often reduce vision from birth, cataracts, glaucoma, corneal keratopathy, and pannus can progressively obscure vision. The consequence of such progressive visual impairments is often blindness in young adulthood [14, 15], necessitating the development of new vision saving therapies. While environmental factors are likely to contribute to the reported variability, epistasis, the non-additive interaction between genetic loci, may also be a factor influencing how the disorder presents, and how it should be treated [16, 17].

The small eye (*Sey*) mouse has a premature termination codon in *Pax6*, mimicking the most frequent aniridia causing mutations. Like human *PAX6* mutations, *Sey* is penetrant, producing a phenotype that mirrors human aniridia: iris hypoplasia, lens abnormalities, corneal keratopathy, and pannus [4, 18–29]. However, the phenotype is highly variable, even between genetically identical mice

Electronic supplementary material The online version of this article (https://doi.org/10.1038/s41434-018-0043-6) contains supplementary material, which is available to authorized users.

✉ Elizabeth M. Simpson
simpson@cmmt.ubc.ca

[1] Centre for Molecular Medicine and Therapeutics at BC Children's Hospital, University of British Columbia, Vancouver, BC, Canada

[2] Department of Medical Genetics, University of British Columbia, Vancouver, BC, Canada

[3] Department of Psychiatry, University of British Columbia, Vancouver, BC, Canada

[4] Department of Ophthalmology and Visual Science, University of British Columbia, Vancouver, BC, Canada

[14, 21, 26, 30, 31]. While mimicking the variability of the human disease state is desirable, variability beyond that seen in humans has also been reported, and may confound the development of new therapeutics [30]. Therefore, identifying and limiting these undesirable sources of variability can help accelerate the development of new treatments for aniridia.

Variability in mouse studies is increased by a myriad of sources. For instance, different mutant alleles of the same gene can impact how a phenotype presents [32]. Similarly, genetic background (bkgd) is an important consideration. Inbred mice are a useful tool, but genetically they deviate considerably from humans, as they are homozygous at all loci, lacking in the diversity found in freely reproducing environments [33–35]. This creates an unnatural situation making some phenotypes frail in a way that does not reflect the biology under study and introduces extraneous variables [30, 36]. Finally, environmental variables such as cage conditions, handling practices, and even the experimenter can increase variability [37–39]. Studies of the *Sey* allele have been conducted on numerous different bkgds and at various timepoints, often focusing on embryonic development. Consequently, before developing new therapeutics for aniridia, it would be beneficial to generate benchmark measurements of the *Sey* phenotype, at a later timepoint more relevant to the treatment of human aniridia. Additionally, it is important that we identify sources of unnatural variation in model organisms, so that new therapies are built around the appropriate underlying biology, not artifacts of the laboratory environment. This helps ensure that outcome measures are relevant to the clinical features targeted for therapy, and minimizes unnecessary variability, which can drive up costs while diminishing the reliability of the findings. Here we pursued the hypothesis that bkgd is a major source of undesirable variability in *Sey* mice.

In this work we investigate how bkgd can introduce variability in the *Sey* mouse, and the underlying mechanism responsible, by conducting a quantitative analysis of the *Pax6*$^{Sey/+}$ (heterozygous (Het)) and *Pax6*$^{Sey/Sey}$ (homozygous (Hom)) phenotypes on three bkgds: C57BL/6J (B6), B6129F1 (F1), and 129S1/SvImJ (129). B6 was selected as C57BL mice are the most commonly studied inbred mouse strain [40–42], serving in numerous *Pax6* studies [23, 24, 43–46]. F1 mice were studied as they are the genetically defined hybrid of B6 and 129 and are often used [34, 47, 48]. 129 was selected as they have been the most commonly used strain for genetic targeting in embryonic stem cells [34, 42]. Rather than searching for modifier genes, we instead looked broadly at how bkgd influences the *Sey* phenotype to address the question: which bkgd should be used for developing new therapies. Examining the eye, brain, and pancreas, we measured and compared anatomical, histological, and molecular aspects of the *Sey* phenotype, and the relationship between *Pax6* genotypes and bkgds. Surprisingly, we found that choice of bkgd can introduce significant variability. We also revealed epistatic interactions between genotype and bkgd, where the resulting phenotype differs from that expected, such that the combination creates a unique or exaggerated phenotype. Using this data, we conclude that the B6129F1 hybrid bkgd is a better choice for therapeutic development than the commonly used inbred strains.

Methods

Mouse husbandry

All mice were bred and maintained in the pathogen-free mouse core facility of the Center for Molecular Medicine and Therapeutics at The University of British Columbia. Animal work was performed in accordance with the guidelines set by the Canadian Council on Animal Care (CCAC) and adhered to the ARVO statement for the use of animals in ophthalmic and vision research. The *Sey* mutation was maintained on inbred C57BL/6J (The Jackson Laboratory (JAX), Stock #000664, Bar Harbor, ME) and 129S1/SvImJ (JAX, Stock #002448) strains of mice backcrossed at least 10 generations. B6129F1 mice were generated by crossing B6 dams to 129 sires to produce F1 progeny. Mice were kept on a 7 am–8 pm light cycle and had food and water *ad libitum* unless stated otherwise.

Adult mice, ages three to six months, were sacrificed by cervical dislocation, imaged under a Leica MZ125 microscope with a CoolSnap-Procf camera (Leica Microsystems, Wetzlar, DE), and the eyes were immediately enucleated. Eyes used for histological examination were prepared as previously described [49]. Briefly, they were enucleated and incubated in 4% PFA at 4°C for 2 h, weighed, transferred to 25% sucrose, and stored at 4°C until used. Eyes used for molecular characterization were placed in room temperature PBS, the cornea and retina were dissected under a dissecting microscope, placed in separate Nunc Cryotubes (MilliporeSigma, St. Louis, MI, Catalog #V7634), flash frozen in liquid nitrogen, and stored at −80°C.

Embryonic day 18.5 (E18.5) fetuses were generated using a previously described timed pregnancy protocol [50]. Het dams and sires were bred, producing *Pax6*$^{+/+}$ (wild type (Wt)), Het, and Hom offspring. On E18.5, pregnant dams were fasted for 2 h, and then sacrificed by cervical dislocation followed by decapitation. Embryos were photographed and then sacrificed by decapitation. Blood glucose readings were immediately taken from sacrificed fetuses, and then brains were dissected and divided along the longitudinal fissure. Each hemisphere was placed into separate Nunc Cryotubes, flash frozen in liquid nitrogen,

and stored at −80°C. Additionally, tail tip samples were taken for genotyping by PCR.

Pax6 genotyping and RT-ddPCR

PCR was performed on genomic DNA from the digested tail tips of E18.5 embryos, and ear notches from adult mice. As there is no literature describing the influence of parent of origin or imprinting on *Pax6*, all Het mice for RNA analysis were bred such that the *Sey* allele came from the sire. Primers were designed to bind to the *Sey* (oEMS6073: CTGAGCTTCATCCGAGTCTTCTTA) and Wt alleles (oEMS6076: AACACCAACTCCATCAGTTCTAATG) on exon 8 of *Pax6*.

RNA was isolated using the QIAGEN AllPrep kit (QIAGEN, Hilden, DE, Catalog #80204), following the provided protocol. RNA integrity and quantity were assessed by the CMMT core sequencing service on Agilent 2100 bioanalyzer RNA 6000 Nano chips (Agilent Technologies, Santa Clara, CA). Reverse transcription was performed using the SuperScript™ VILO™ cDNA Synthesis Kit and Master Mix (Thermo Fisher Scientific, Waltham, MA, Catalog # 11754050) as directed. For reverse transcriptase Droplet Digital PCR (RT-ddPCR) cDNA was diluted to a standard concentration of 0.1 ng and tested on a QX100 Droplet Digital PCR system (Bio Rad, Hercules, CA) as directed. Custom Taqman primers with specificity to either the *Sey* (*Sey* assay) or wild-type (Wt assay) allele were designed. For both assays the forward primer binds to exon 7 (oEMS6130: ACTTCAGTACCAGGGCAAC) and the probe binds to exon 8 (oEMS6131: AACTGATGGAGTTGGTGTTCTCTCCC). The reverse primers for the *Sey* (oEMS6132: GAGCTTCATCCGAGTCTTCTTA) and Wt (oEMS6133: GAGCTTCATCCGAGTCTTCTTC) assays bind to exon 8, with the 3′ end complementary to the *Sey* or Wt allele, respectively, with the exception of a mismatch at the 3′ penultimate nucleotide, which was intentionally introduced to improve the specificity of the assay as previously described [51]. *Pax6* transcript measurements were normalized to the geometric mean of three housekeeping genes using commercially available assays: *Pgk1*, *B2m*, and *Tfrc* (Integrated DNA Technologies, Coralville, IO, Assay# Mm.PT.39a.22214854, Mm.PT.58.10497647, and Mm.PT.58.9333140, respectively) [52].

Western blotting

As there is no literature describing the influence of parent of origin or imprinting on *Pax6*, all Het mice for protein analysis were bred such that the *Sey* allele came from the sire. Proteins were extracted by homogenizing tissue for 30 s in radioimmunoprecipitation assay buffer (150 mM sodium chloride, 1.0% sodium deoxycholate, 1.0% nonyl phenoxypolyethoxylethanol, 0.1% sodium dodecyl sulfate, & 25 mM Tris pH 7.8) containing 1% cOmplete™ protease inhibitor (Roche Diagnostics GmbH, Mannheim, DE, Catalog # 11 697 498 001), 1% phenylmethylsulfonyl fluoride (MilliporeSigma, Catalog # P7626), and 1% sodium orthovanadate (MilliporeSigma, Catalog # P6508). Homogenates were sonicated 2 × for 10 s, rotated for 15 min at 40 °C, and spun down. Supernatant was transferred to a fresh tube and stored at − 80°C. Protein samples were quantified using a DC Protein kit (Bio Rad, Catalog# 500–0113, 500–0114, 500–0015) as directed. For E18.5 brains, adult retinas, and adult corneas, 29, 6.5, and 3.4 µg of protein, respectively, were assessed by western blot using the NuPAGE gel and buffer system (Thermo Fisher Scientific, Catalog# NP0341BOX, NP0002, NP0005, NP0006-1, NP0008, & NP0009), Immun-Blot PVDF Membranes (Bio Rad; Catalog # 162–0255), and the XCell II Blot Module (Thermo Fisher Scientific, Catalog # EI9051) as directed. Membranes were blocked for 1 h in 5% skim milk (Becton, Dickson, and company, Franklin Lakes, NJ, Catalog # DF0032173) labeled with antibodies against PAX6 (7.5:10,000; Biolegend, San Diego, CA, Catalog # 901301) and Lamin B1 (7.5:10,000; Santa Cruz Biotechnology, Dallas, TX, Catalog # sc-30264) overnight at 4°C, labeled with secondary antibodies against Rabbit (1:5000; Thermo Fisher Scientific, Catalog # A10043) and Goat (1:5000; Rockland, Limerick, PA, Catalog # 605-731-002) and imaged on a LiCOR Odyssey (Li-COR Biosciences, Lincoln, NE). PAX6 measurements were standardized to Lamin β1 measurements. Lanes where the blotting was weak, with Lamin β1 below 2000 arbitrary units, were excluded from analysis.

Histological analysis

As there is no literature describing the influence of parent of origin or imprinting on *Pax6*, Het mice for histological analysis were bred such that the *Sey* allele was inherited from either the sire or the dam. As expected, our data showed no influence of parent of origin by one-way analysis of variance (ANOVA). Eyes were embedded, sectioned, and stained with Hoechst as previously described [50]. Imaging was performed on a Leica SP8 Confocal microscope (Leica Microsystems) at 40x magnification and raw image files were converted to composite tagged image file format (TIFF) files using ImageJ software (http://imagej.nih.gov/ij/, version 1.48) with the Bio-Formats plugin (http://www.openmicroscopy.org/site/support/bio-formats5.1/users/imagej/). Tiling images of whole eyes were taken using a Bx61 fluorescent microscope (Olympus Corporation, Tokyo, JP) and saved as TIFFs using ImageJ.

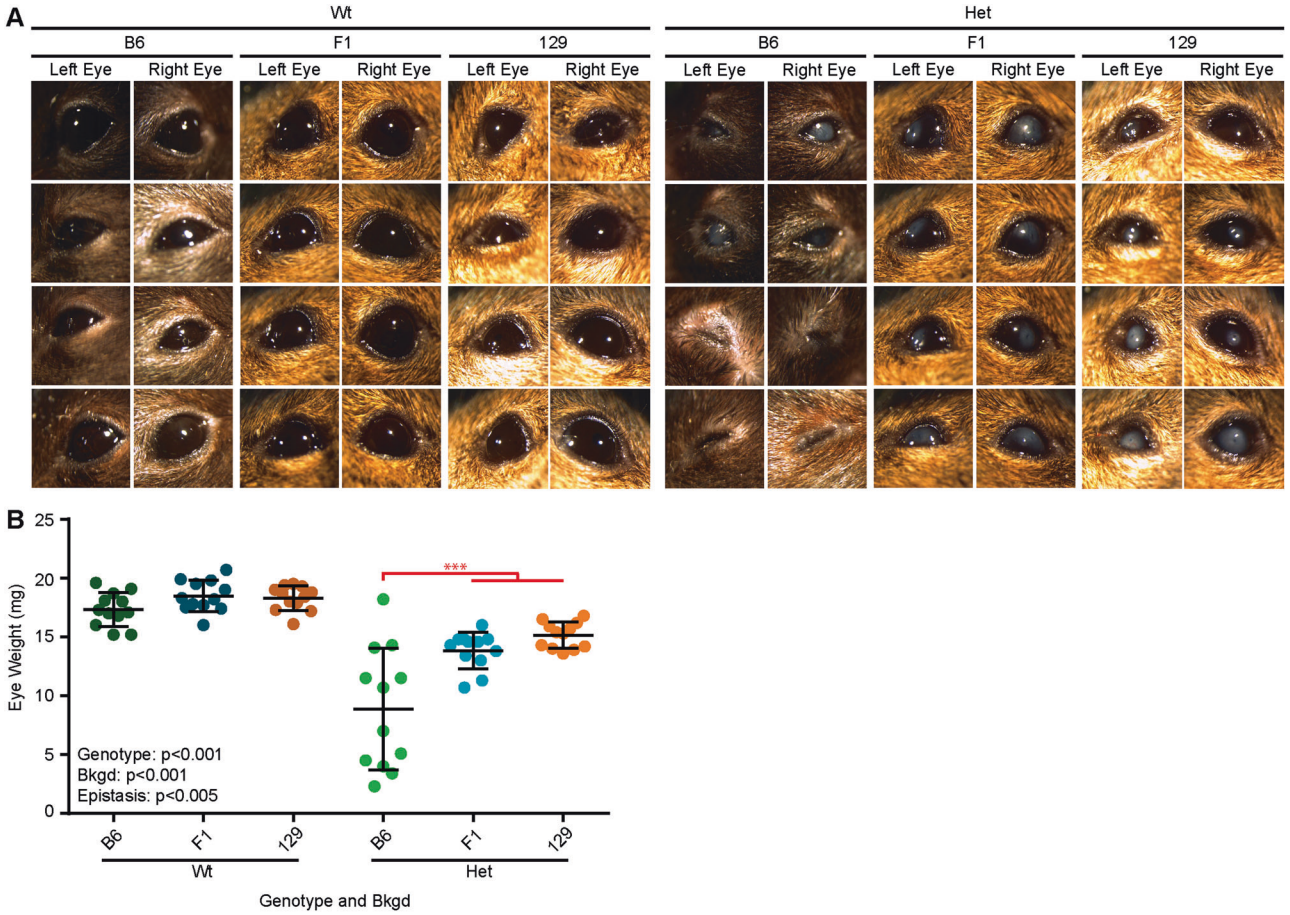

Fig. 1 Epistasis produced a severe microphthalmia phenotype in Het B6 eyes. **a** Images of *Pax6*$^{+/+}$ (Wt) and *Pax6*$^{Sey/+}$ (Het) mouse eyes on three genetic backgrounds (bkgds), C57BL/6J (B6), B6129F1 (F1), and 129S1/SvImJ (129), were examined under a light microscope. Some Het eyes on the B6 bkgd displayed a more severe microphthalmia phenotype where only a very small eye could be detected after manually opening the eyelids with forceps. **b** Weight of enucleated eyes was quantified after fixation. *Pax6* genotype and bkgd were both found to influence eye weight. Epistasis between *Pax6* genotype and bkgd was also discovered, and indicated on the graph (red). *Post hoc* analysis revealed that Het B6 eyes were significantly lighter than Het F1 or 129 eyes (***$p < 0.001$ for both). Statistical significance was determined using ANOVA, *post hoc* analysis was performed using Fisher's LSD with Bonferroni's correction for multiple comparisons. Each dot represents an individual eye and error bars represent the mean ± the standard deviation

Cell counting and thickness measurements were done blinded to genetic background and *Pax6* genotype. For each eye, three non-overlapping images were taken for analysis, all within 500 µm of the optic nerve for the retina, or above the pupil for the cornea. In the cornea, structural abnormalities such as keratolenticular adhesions were excluded from measurements. Counts were performed manually using the cell counter tool in ImageJ. All cells in the ganglion cell layer were counted, while the number of cells in the inner and outer nuclear layers was calculated by counting one vertical row of cells in the center of each window, and one horizontal row of cells along the edge of the layer. The vertical and horizontal counts were then multiplied together to give an estimate of the cell number, per layer, in a 200 µm window of the retina. Measurements and counts from three images were averaged to produce final figures for each animal. Four different animals were used for each genotype and bkgd. Images of embryonic eyes were examined blinded to genotype and bkgd. For measurements of embryonic whole eye area and non-pigmented area, both were manually circled, and the corresponding areas were calculated using ImageJ.

Statistical analysis and data presentation

Sample sizes were based on similar experiments in the literature [23, 44, 53]. All data were analyzed using a two-way ANOVA, performed using IBM SPSS version 24 (SPSS Inc., Chicago, IL). Normality of residuals and variance was assessed using Shapiro–Wilk test and Levene test, respectively. Variance was found to be equal for 16 of 24 datasets. In the eight instances where the assumption of equal variance was violated (eye weight, cornea stroma/endothelial cell count, E18.5 brain Wt-specific mRNA,

E18.5 brain Sey-specific mRNA, adult retina Sey-specific mRNA, cornea Sey-specific mRNA, cornea Non-specific mRNA, and blood glucose), we proceeded to run the two-way ANOVA as ANOVA is robust to moderate differences in variability when the sample sizes are equal, as they are in these cases [54]. Main effects of the ANOVA were reported and when significant differences between *Pax6* genotypes and bkgds were found, Tukey's honest significant difference *post hoc* test was performed. If a significant interaction was discovered, Fisher's least significant difference *post hoc* test was performed, and Bonferroni's correction was applied to α, to determine where significant interactions occurred. All results are reported as the mean ± standard deviation to reflect the variability within the assays used and the measurements taken. Blood glucose measurements were replicated in two separate cohorts of mice, all other measurements were taken once. Graphs were generated using GraphPad Prism version 6 (GraphPad Software Inc., La Jolla, CA). Each data point is represented by a dot; each genetic background is presented in a different color: B6 (green), F1 (blue), 129 (orange); and each genotype is represented by different shading: Wt (dark), Het (medium), and Hom (light). Error bars represent the standard deviation around the mean for each measure. To facilitate use of this data for benchmarking and power calculations, means and standard deviations for all quantitative measurements were reported in the supplementary tables.

Results

Epistasis between the *Pax6* genotype and bkgd influenced eye weight

The Het phenotype was apparent by visual inspection of adult Wt and Het mice on all three bkgds (Fig. 1a), confirming the stability of the classic phenotype: microphthalmia, central corneal clouding, and corneal vascularization. However, exclusively in B6 mice, a subset of Het mice presented with severe microphthalmia, where the eye was so small that it resembled anophthalmia, as no eye was externally visible, and the eyelids were closed (often a very small eye could be found by manually opening the eyelids). The Het phenotype was quantified by measuring eye weight after enucleation (Table S1). Two-way ANOVA confirmed that *Pax6* genotype and bkgd ($p < 0.001$ for both) both influenced eye weight, where B6 eyes were found to be significantly lighter than F1 and 129 eyes ($p < 0.001$ for both) (Fig. 1b and Fig. S1). Furthermore, a significant epistatic interaction between *Pax6* genotype and bkgd was also found ($p < 0.005$), where B6 Het eyes were significantly smaller than F1 or 129 Het eyes ($p < 0.001$ for both).

Such bkgd-specific differences could have developmental origins, therefore we examined the eyes of Wt, Het, and Hom embryos. As Hom mice only survive until shortly after birth, samples were collected at E18.5. Immediately, the influence of *Pax6* genotype was apparent, as Wt embryos had larger eyes with larger pupils than Het eyes, while Hom embryos presented with anophthalmia and a shortened snout (Fig. S2A). The size of the embryonic whole eye area was estimated using the circumference of the pigmented ring (Table S2). Two-way ANOVA revealed that *Pax6* genotype and bkgd($p < 0.001$ for both) both significantly influenced embryonic eye size, where 129 embryos had significantly smaller eyes than B6 and F1 embryos ($p < 0.005$ for both) and that B6 embryos had smaller eyes than F1 ($p < 0.005$) (Fig. S2B and Fig. S3). Furthermore, a significant epistatic relationship between *Pax6* genotype and bkgd was also found ($p < 0.05$) where Wt 129 embryos had significantly smaller eyes than Wt B6 ($p < 0.005$) and Wt F1 embryos ($p < 0.001$), and Het F1 embryos had larger eyes than Het 129 embryos ($p < 0.001$). Measurements of Hom eyes were not taken, as no distinguishable ocular structure could be detected. In addition to eye size, a difference in the non-pigmented area, pupil, was also observed by visual inspection. Quantification revealed that *Pax6* genotype and bkgd ($p < 0.001$ for both), where B6 embryos had significantly smaller non-pigmented areas than F1 or 129 embryos ($p < 0.001$ for both) (Fig. S2C). No epistatic interactions were found.

Overall, the gross morphology suggested that a closer inspection of ocular tissues was warranted to determine how these gross differences influence the finer structures of the eye.

Genetic background influenced retinal thickness

Cryosections from the center of the eyes (defined as cross sections containing the optic nerve) were stained with Hoechst and imaged under a fluorescent microscope. Qualitatively, these images support the gross morphological data, where the reduction in eye weight of Het mice corresponds to a reduction in eye size in all three bkgds (Fig. S4). Additionally, sections of severely microphthalmic eyes revealed major structural perturbations including: anterior synechia, lens hypoplasia or aphakia, and retina dysplasia. The extreme retinal malformations in these eyes made accurate quantification of the retina, and microdissection for RNA and protein extraction, challenging. Thus, such eyes were excluded from the remainder of the study.

To explore how *Pax6* genotype and bkgd influence the structure of the retina, confocal images were taken of the central retina (within 500 µm of the optic nerve) (Fig. 2a). Retinal thickness and cell number were quantified

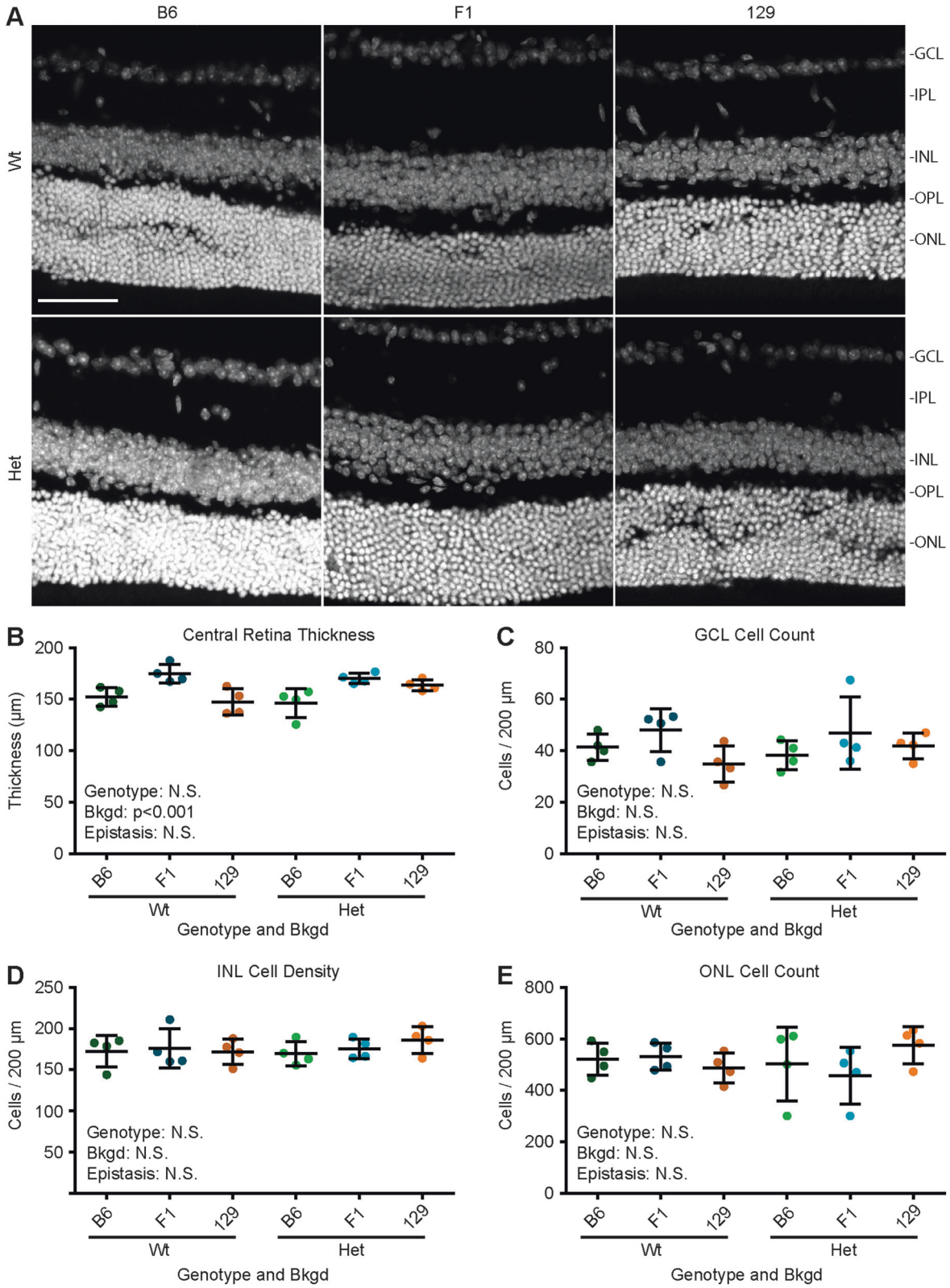

(Table S3). ANOVA revealed that bkgd ($p < 0.005$), but not *Pax6* genotype or epistasis, influenced retinal thickness (Fig. 2b), where F1 mice had significantly thicker retinas than B6 ($p < 0.001$) and 129 mice ($p < 0.005$). Cell numbers in each layer were also estimated within a 200 µm window of the central retina, and no significant differences were

◀ **Fig. 2** Genetic background, but not *Pax6* genotype, influenced retinal thickness. **a** Confocal scans of $Pax6^{+/+}$ (Wt) and $Pax6^{Sey/+}$ (Het) retinas on three genetic backgrounds (bkgds), C57BL/6J (B6), B6129F1 (F1), and 129S1/SvImJ (129). **b** Quantifying retinal thickness revealed that *Pax6* genotype had no influence, but bkgd significantly influenced retinal thickness. Neither *Pax6* genotype nor bkgd were found to influence cell count for the (**c**) ganglion cell layer (GCL), (**d**) inner nuclear layer (INL), or (**e**) outer nuclear layer (ONL). Gray staining (Hoechst), inner plexiform layer (IPL), outer plexiform layer (OPL), not significant (N.S.), scale bar = 50 µm. Statistical significance was determined using ANOVA, *post hoc* analysis was performed using Fisher's LSD with Bonferroni's correction for multiple comparisons. Each dot represents an individual eye and error bars represent the mean ± the standard deviation

found in the ganglion cell layer (Fig. 2c), inner nuclear layer (Fig. 2d), or outer nuclear layer (Fig. 2e).

Epistasis between *Pax6* genotype and genetic background influenced corneal thickness

To explore how the structure of the cornea is influenced by *Pax6* genotype and bkgd, confocal images were taken of the central cornea above the pupil, excluding keratolenticular adhesions (Fig. 3a). Measurements of corneal thickness and cell number were taken (Table S4). ANOVA revealed that *Pax6* genotype and bkgd($p < 0.001$ for both), where 129 mice had thicker cornea epithelia than B6 and F1 mice ($p < 0.005$ and $p < 0.001$, respectively) (Fig. 3b and Fig. S5). Furthermore, a significant epistatic interaction between *Pax6* genotype and bkgd was also found ($p < 0.05$) where Het 129 mice had thicker cornea epithelia than Het B6 ($p < 0.005$) and Het F1 ($p < 0.001$). Similarly, *Pax6* genotype and bkgd influenced the number of cells in the corneal epithelium, where 129 mice had more epithelial cells than B6 and F1 mice ($p < 0.001$ for both) (Fig. 3c and Fig. S6). Furthermore, a significant epistatic interaction between *Pax6* genotype and bkgd was found, where Het 129 mice had more epithelial cells than Het B6 and Het F1 mice ($p < 0.001$ for both).

Examining the corneal stroma and endothelium, ANOVA revealed that *Pax6* genotype ($p < 0.001$), but not bkgd or epistasis, influenced thickness, as the stroma and endothelium of Wt mice was thicker than that of Het mice (Fig. 3d). Conversely, while *Pax6* genotype ($p < 0.05$) also influenced the number of stromal cells, the stroma of eyes from Wt mice had significantly fewer cells than Het mice (Fig. 3e).

Epistasis between *Pax6* genotype and genetic background influenced *Pax6* mRNA transcript levels

Underlying the ocular phenotype of all Het and Hom mice is PAX6 haploinsufficiency, caused by the *Sey* mutation. Therefore, it could be that differences in PAX6 mRNA and/or protein levels could be the mechanism(s) causing the bkgd-specific differences. This prompted us to investigate the molecular phenotype of these mice. Beginning with mRNA, three RT-ddPCR assays were developed to interrogate *Pax6* mRNA transcript levels. The first two assays specifically amplified either the Wt or *Sey* allele of *Pax6*, while the third was not allele-specific and amplified regions of exons 8 and 9, beyond the *Sey* mutation. As Hom mice do not develop eyes, the brains of E18.5 embryos were used. The same assays were then applied to mRNA from more therapeutically relevant tissues: the adult retina and cornea. Transcript levels for all assays and tissues were reported in Table S5.

In the E18.5 brain, ANOVA revealed that *Pax6* genotype ($p < 0.001$), but not bkgd or epistasis, influenced Wt-specific *Pax6* transcript levels (Fig. 4a), where Wt embryos had significantly higher Wt-specific *Pax6* transcript levels than brains from Het embryos ($p < 0.001$) and brains from both Wt and Het embryos had significantly higher levels than brains from Hom embryos ($p < 0.001$ for both). *Pax6* genotype alone ($p < 0.001$), also significantly influenced the amount of *Sey*-specific mRNA levels (Fig. 4b), where Wt embryos had significantly fewer *Sey* transcripts than Het embryos ($p < 0.005$) and that both Wt and Het embryos had significantly fewer *Sey* transcripts than Hom embryos ($p < 0.001$). Similarly, *Pax6* genotype ($p < 0.001$) and bkgd ($p < 0.05$), both significantly influenced non-specific *Pax6* mRNA levels (Fig. 4c), where Hom embryos had significantly higher *Pax6* transcript levels than Wt and Het embryos ($p < 0.001$ for both). Additionally, it was found that B6 embryos had significantly fewer *Pax6* transcripts than brains from 129 embryos ($p < 0.05$).

In the adult retina, *Pax6* genotype and bkgd ($p < 0.001$ for both) both significantly influenced Wt-specific *Pax6* transcript levels (Fig. 4d and Fig. S7), where B6 mice had significantly lower Wt-specific *Pax6* mRNA levels than 129 retinas ($p < 0.01$). Furthermore, a significant epistatic interaction between *Pax6* genotype and bkgd was found ($p < 0.05$), where Wt B6 mice had significantly lower Wt-specific *Pax6* transcript levels than retinas from Wt F1 and Wt 129 mice ($p < 0.005$ and $p < 0.001$, respectively), and that retinas from Het B6 mice had significantly lower Wt-specific *Pax6* transcript levels than retinas from Het 129 mice ($p < 0.05$). Similarly, *Pax6* genotype ($p < 0.001$) and bkgd ($p < 0.05$) both significantly influenced *Sey*-specific *Pax6* transcript levels, revealing B6 mice had lower *Sey*-specific *Pax6* transcript levels than retinas from 129 mice ($p < 0.05$) (Fig. 4e and Fig. S8). Furthermore, a significant epistatic interaction between *Pax6* genotype and bkgd was also found ($p < 0.05$), revealing that retinas from Het B6 mice had lower *Sey*-specific *Pax6* transcript levels than retinas from Het 129 mice ($p < 0.005$). Finally, *Pax6* genotype ($p < 0.001$) and bkgd ($p < 0.005$), but not epistasis,

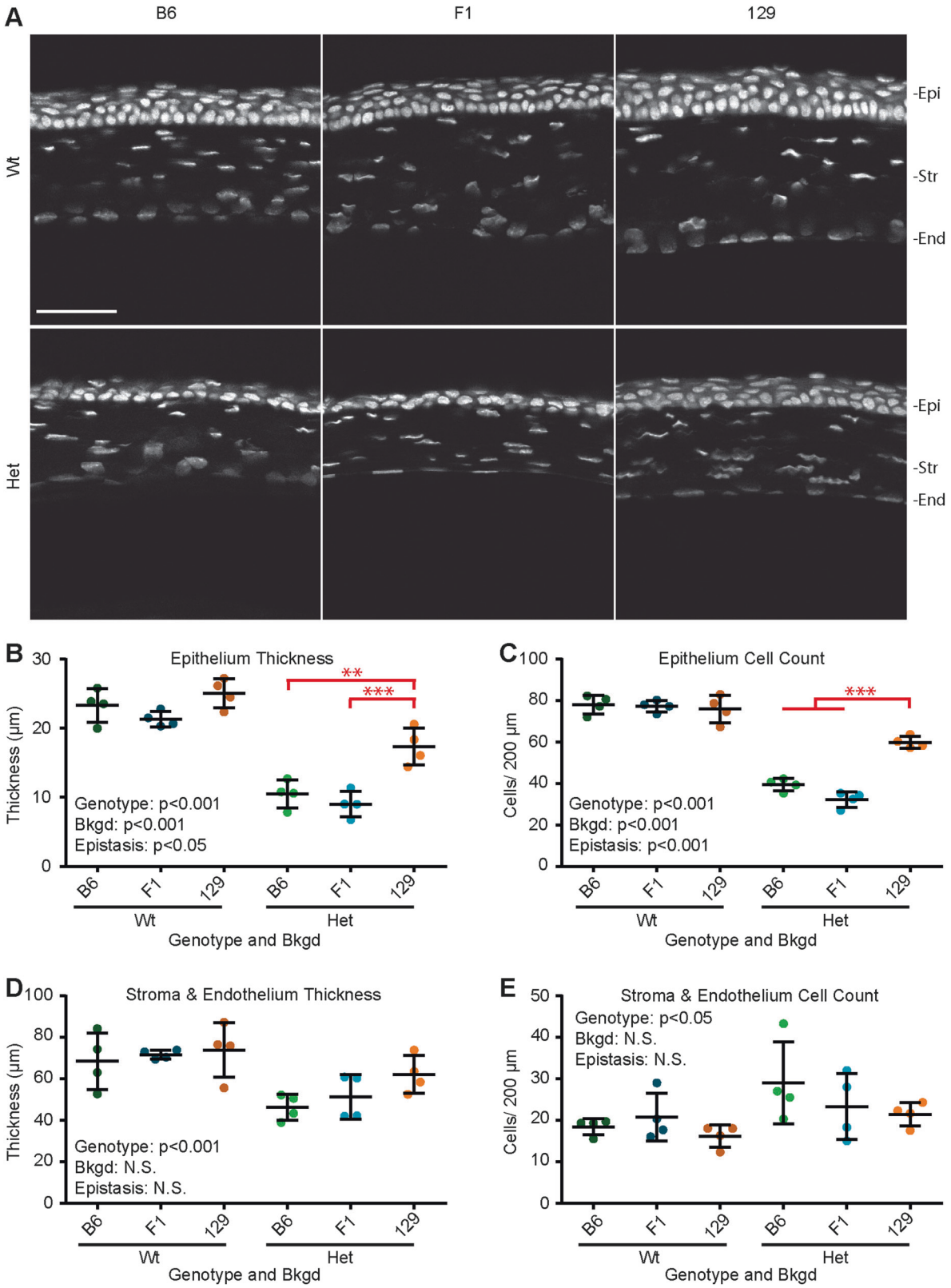

influenced non-specific *Pax6* transcript levels (Fig. 4f), revealing that retinas from Het B6 mice had lower non-specific *Pax6* transcript levels than retinas from Het F1 ($p < 0.05$) and Het 129 ($p < 0.005$).

In the adult cornea, similar patterns to the retina were observed, where *Pax6* genotype ($p < 0.001$), and bkgd ($p < 0.05$), but not epistasis, influenced Wt-specific *Pax6* transcript levels, from F1 ($p < 0.005$) and 129 mice ($p < 0.05$)

◀ **Fig. 3** Epistasis influenced corneal epithelial thickness and cell counts. **a** Confocal scans of $Pax6^{+/+}$ (Wt) and $Pax6^{Sey/+}$ (Het) corneas on three genetic backgrounds (bkgds), C57BL/6J (B6), B6129F1 (F1), and 129S1/SvImJ (129) were examined. Quantification of (**b**) cornea epithelium (Epi) thickness, (**c**) Epi cell count, (**d**) stroma (Str) plus endothelial (End) thickness, and (**e**) Str plus End cell count, revealed that *Pax6* genotype influenced all measurements. Additionally, epistasis between *Pax6* genotype and bkgd influenced Epi thickness and cell count. *Post hoc* analysis of epistasis, indicated on graphs (red), revealed that Het 129 corneas had significantly thicker Epi than Het B6 and Het F1 corneas (**$p < 0.005$, and ***$p < 0.001$, respectively), and that Het 129 corneas had more Epi cells than Het B6 and Het F1 corneas ($p < 0.001$ for both). Gray staining (Hoechst), not significant (N.S.), scale bar = 50 µm. Statistical significance was determined using ANOVA, *post hoc* analysis was performed using Fisher's LSD with Bonferroni's correction for multiple comparisons. Each dot represents an individual eye and error bars represent the mean ± the standard deviation

(Fig. 4g). *Pax6* genotype ($p < 0.001$), but not bkgd or epistasis, influenced the levels of *Sey*-specific *Pax6* transcripts (Fig. 4h). *Pax6* genotype ($p < 0.001$) and bkgd ($p < 0.005$), but not epistasis, influenced non-specific *Pax6* transcript levels, revealing that B6 mice had lower non-specific *Pax6* transcript levels than corneas from 129 mice ($p < 0.005$) (Fig. 4i).

Pax6 genotype influenced PAX6 protein levels

As bkgd influenced *Pax6* mRNA transcript levels, we proceeded to determine if those differences translated to the protein level using western blotting. As expected, blots of protein samples from E18.5 mouse brains reveled a qualitative reduction in PAX6 band intensity between Wt, Het, and Hom mice (Fig. 5a). Western blots were quantified (Table S6), and ANOVA revealed *Pax6* genotype ($p < 0.001$), but not bkgd or epistasis, influenced PAX6 protein levels (Fig. 5b), revealing that brains from Wt embryos had more protein than brains from Het and Hom embryos ($p < 0.001$ for both). Similarly, protein samples taken from adult mouse retinas (Fig. 5c, d), and corneas (Fig. 5e, f) revealed that *Pax6* genotype ($p < 0.001$ and $p < 0.005$, respectively), but not bkgd or epistasis influenced PAX6 protein levels, and that samples from Wt retina and corneas had more PAX6 protein than retinas and corneas from Het mice.

Epistasis between *Pax6* genotype and bkgd influenced blood glucose levels

To quantify how the *Sey* mutation influences pancreas function, blood glucose measurements were taken from E18.5 Wt, Het, and Hom mouse embryos from each bkgd (Table S7). *Pax6* genotype and bkgd, were both found to significantly influence blood glucose levels, revealing that Hom embryos had higher blood glucose levels than Wt ($p < 0.005$) and Het embryos ($p < 0.001$), F1 embryos had higher blood glucose levels than B6 and 129 ($p < 0.001$ for both), and that B6 embryos had higher blood glucose levels than 129 embryos ($p < 0.001$) (Fig. 6 and Fig. S8). Furthermore, a significant epistatic interaction between *Pax6* genotype and bkgd was found ($p < 0.001$), revealing that Wt F1 embryos had higher blood glucose levels than Wt B6 and Wt 129 embryos ($p < 0.001$ for both), Het 129 embryos had significantly lower blood glucose levels than Het B6 and Het F1 embryos ($p < 0.001$ for both), Hom F1 embryos had higher blood glucose levels than Hom B6 and Hom 129 embryos ($p < 0.001$ for both), and Hom B6 embryos had higher blood glucose levels than Wt 129 embryos ($p < 0.001$).

Discussion

We have contributed substantially to the general knowledge of *PAX6* null alleles by performing a systematic examination of the Het and Hom phenotypes across multiple bkgds. Consistently, the *Sey* allele produced microphthalmia, decreased corneal epithelial thickness, reduced ocular *Pax6* mRNA levels, and reduced PAX6 protein levels. Surprisingly, we made the novel discovery that the *Sey* allele does not decrease retinal thickness in Het mice, conflicting with previous descriptions of Het B6 eyes [23, 24]. This could be due to our exclusion of Het B6 eyes with severe microphthalmia, where extreme retinal malformations are apparent upon histological examination, making accurate quantification challenging. Our study also revealed thinning of the corneal stroma in Het eyes. Conversely, a previous study reported stromal thickening in Het mice carrying the $Pax6^{Sey\text{-}Neu}$ allele on an unspecified background. However, the authors of that study questioned if this was a biological finding, or a technical artifact [18].

Typically, mRNA transcripts containing premature termination codons are degraded by nonsense mediated decay (NMD) [55], and *Pax6* is known to be subject to NMD in both humans [56–58] and mice [59]. It is known that compensatory mechanism can help rescue deleterious mutations [60–62]. Specifically, previous in situ hybridization studies detected *Pax6* mRNA in Hom *Sey* brains [63, 64]. Our results support NMD for *Pax6* in the adult retina and cornea. Surprisingly, we discovered this was not the case in embryonic brains, where Hom embryos had the highest levels of *Pax6* mRNA. One explanation for the elevated levels of *Sey* transcripts in the embryonic mouse brains might be suppression of NMD [65, 66]. However, the Hom embryos had approximately five times more *Sey* transcripts than Het embryos, which suggests that there is a mechanism beyond NMD suppression. Interestingly, in Het

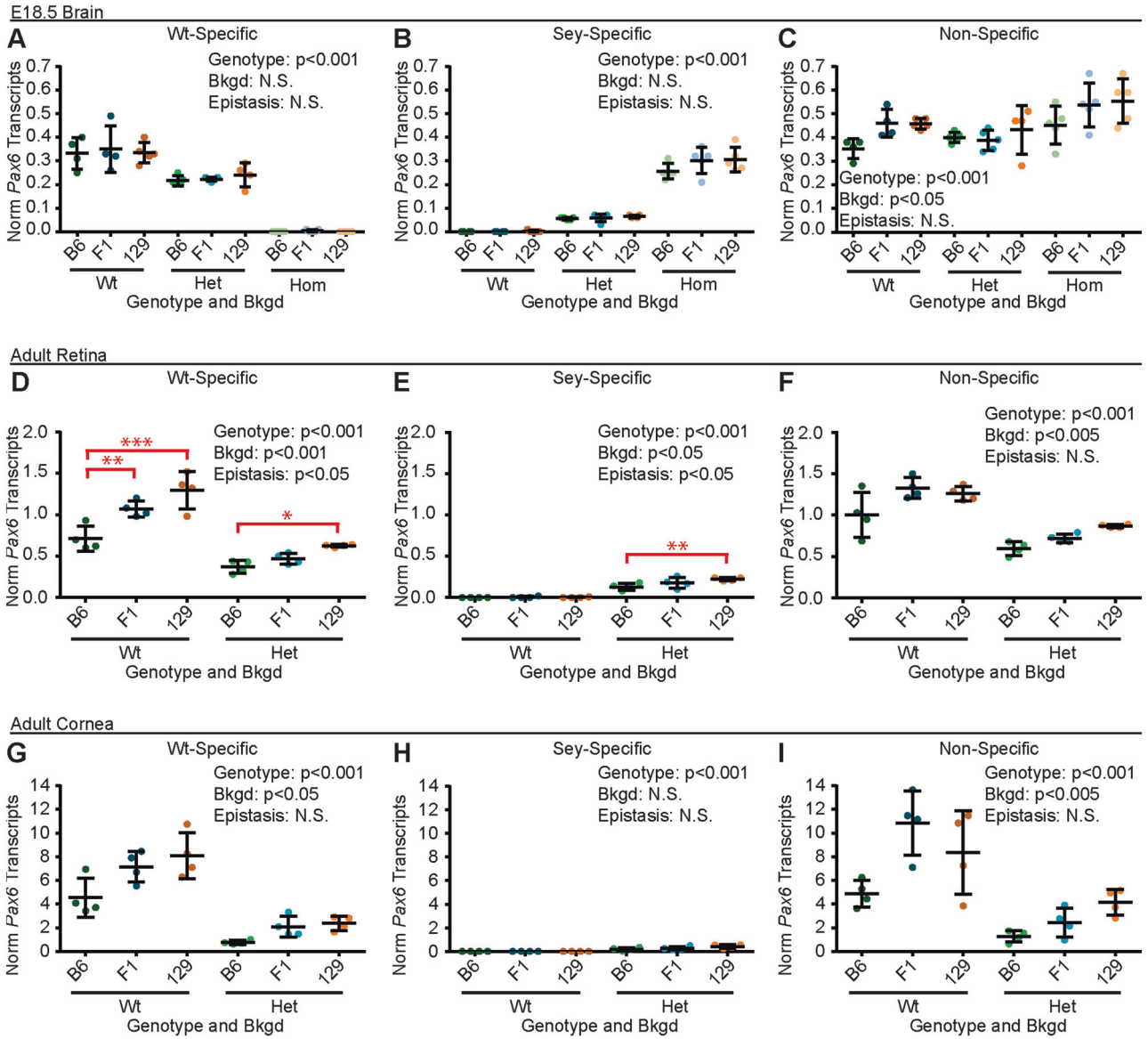

Fig. 4 Epistasis influenced adult *Pax6* mRNA levels. *Pax6* mRNA transcripts from (**a**–**c**) embryonic day 18.5 (E18.5) brains, (**d**–**f**) adult retinas, and (**g**–**i**) adult corneas of *Pax6*$^{+/+}$ (Wt), *Pax6*$^{Sey/+}$ (Het), *Pax6*$^{Sey/Sey}$ (Hom; E18.5 brains only), were measured on three genetic backgrounds (bkgds): C57BL/6J (B6), B6129F1 (F1), and 129S1/SvImJ (129). Three RT-ddPCR assays were used to measure Wt (Wt-specific), *Sey* (Sey-specific), and both Wt and *Sey* combined (non-specific) *Pax6* transcript levels. *Pax6*-genotype was found to influence Wt-, Sey-, and Non-specific *Pax6* transcript levels in all tissues. Similarly, bkgd influenced at least one *Pax6* transcript levels in all tissues. Epistasis between *Pax6* genotype and bkgd was also measured in retinal mRNA samples, and indicated on the graphs (red). For Wt-specific *Pax6* transcripts, *post hoc* analysis revealed that retinas from Wt B6 mice had lower transcript levels than retinas from Wt F1 and Wt 129 mice (**$p < 0.005$ and ***$p < 0.001$; respectively) and retinas from Het B6 mice had significantly lower Wt-specific *Pax6* transcript levels than retinas from Het 129 mice ($p < 0.05$). *Post hoc* analysis of Sey-specific *Pax6* transcripts also revealed that retinas from Het B6 mice had lower Sey-specific *Pax6* transcript levels than retinas from 129 mice ($p < 0.005$). Not significant (N.S.). Statistical significance was determined using ANOVA, *post hoc* analysis was performed using Fisher's LSD with Bonferroni's correction for multiple comparisons. Each dot represents an individual mouse and error bars represent the mean ± the standard deviation

embryos, Wt-specific *Pax6* mRNA levels were also higher than expected; greater than 50% of Wt embryo levels. Together, these findings suggest that a compensatory mechanism is acting upon Wt and *Sey* alleles or transcripts, boosting *Pax6* transcription or transcript levels during the development of Het and Hom embryos. While PAX6 autoregulation has been previously reported [67], this does not seem to be the mechanism observed here, since Hom mice with no functional PAX6, have the highest transcript levels [65, 66]. Therefore, we hypothesize that a

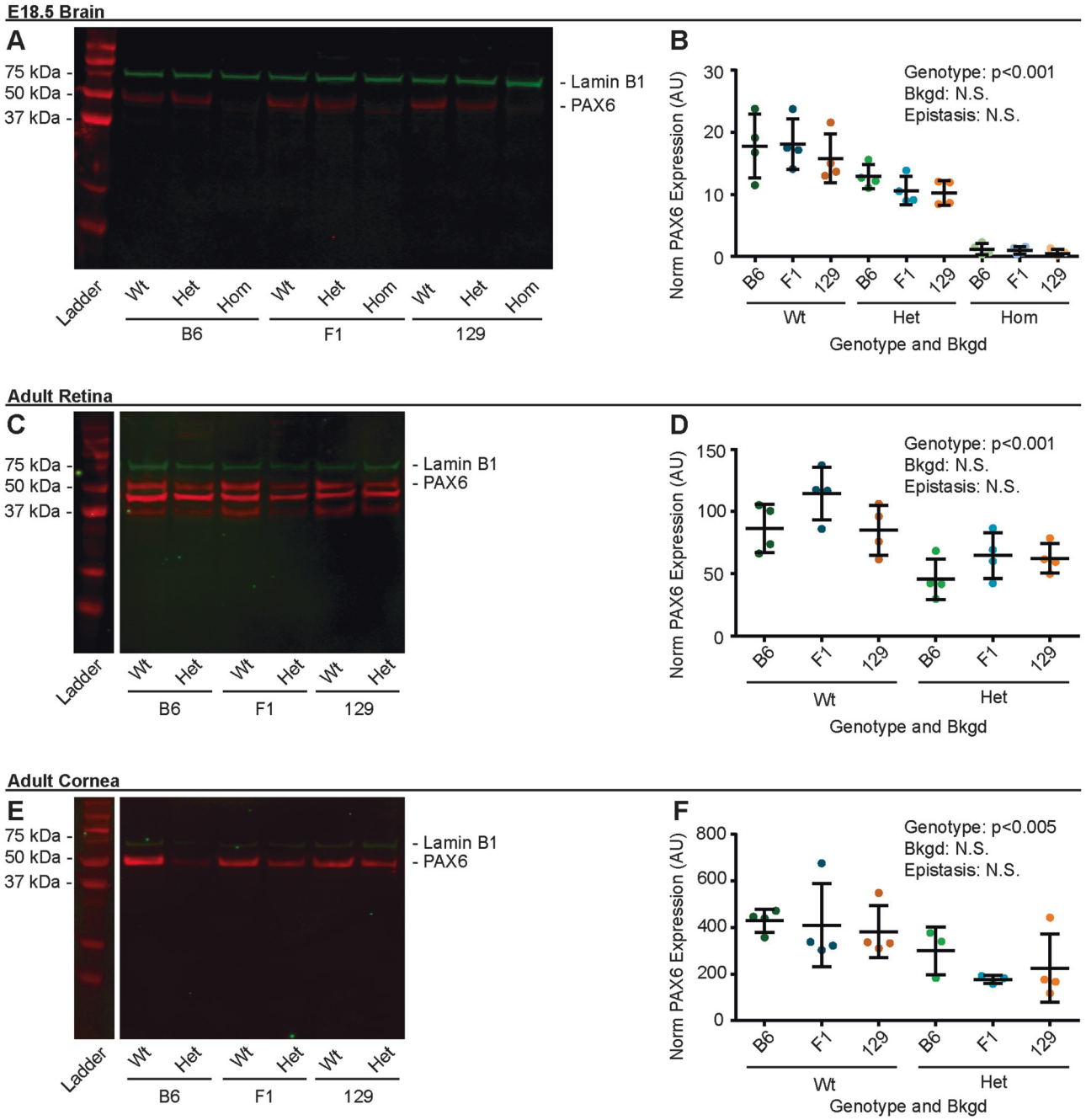

Fig. 5 Only *Pax6* genotype influenced PAX6 protein levels. PAX6 protein from **a** and **b** embryonic day 18.5 (E18.5) brains, **c** and **d** adult retinas, and **e** and **f** adult corneas of $Pax6^{+/+}$ (Wt), $Pax6^{Sey/+}$ (Het), $Pax6^{Sey/Sey}$ (Hom; E18.5 brains only), was measured by western blot on three genetic backgrounds (bkgds): C57BL/6J (B6), B6129F1 (F1), and 129S1/SvImJ (129). Genotype was found to influence PAX6 protein levels in all tissues examined. PAX6 immunostaining (red), Lamin B1 immunostaining (green), arbitrary units (AU), not significant (N.S.). Statistical significance was determined using ANOVA. Each dot represents an individual mouse and error bars represent the mean ± the standard deviation

development-specific mechanism, which does not depend on functional PAX6, drives compensatory *Pax6* transcription in embryonic mouse brains.

In all tissues tested, the influence of mouse bkgd was detected, resulting in differences in eye weight, retinal thickness, corneal thickness, *Pax6* mRNA levels, and blood glucose levels. In the eye, the B6 bkgd introduced considerable variability, with eyes varying from severe to moderate microphthalmia and severe to moderate structural perturbations. As microphthalmia is very rarely reported in aniridia [68–70], and in some cases is thought to be caused by mutations in other important eye genes such as *SOX2*

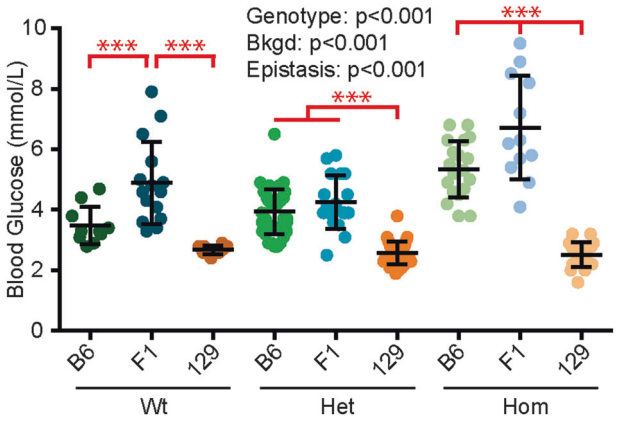

Fig. 6 Epistasis influenced embryonic blood glucose levels. Blood glucose from *Pax6*$^{+/+}$ (Wt), *Pax6*$^{Sey/+}$ (Het), *Pax6*$^{Sey/Sey}$ (Hom) embryonic day 18.5 brains was measured on three genetic backgrounds (bkgds): C57BL/6J (B6), B6129F1 (F1), and 129S1/SvImJ (129). Genotype and bkgd was found to influence blood glucose levels. Epistasis between *Pax6* genotype and bkgd also influenced blood glucose levels, as indicated on graph (red). *Post hoc* analysis revealed that Wt F1 embryos had significantly higher blood glucose levels than Wt B6 and Wt 129 embryos (***$p < 0.001$ for both). It was also revealed that Het 129 embryos had significantly lower blood glucose levels than Het B6 and Het F1 embryos ($p < 0.001$ for both). Finally, Hom F1 embryos had significantly higher blood glucose levels than Hom B6 and Hom 129 embryos ($p < 0.001$), and Hom B6 embryos had higher blood glucose levels than Wt 129 embryos ($p < 0.001$). Statistical significance was determined using ANOVA, *post hoc* analysis was performed using Fisher's LSD with Bonferroni's correction for multiple comparisons. Each dot represents an individual embryo and error bars represent the mean ± the standard deviation

and *OTX2* in addition to the aniridia causing *PAX6* mutation [71, 72]. Therefore, severe microphthalmia is not an ideal phenotype to study for treatment of aniridia. Furthermore, such a severe phenotype, that does not mimic typical aniridia, represents a danger to therapeutic development. The increased variability can bias results, drive up experimental cohorts, and threaten reproducibility, underscoring why the choice of bkgd is critical.

Our discovery of epistasis between *Pax6* genotype and the B6 and 129 bkgds, producing severe microphthalmy and suppressed blood glucose levels, respectively, is congruent with earlier reports that Wt C57BL/6 mice spontaneously develop microphthalmia [73], and that Wt 129 Sv mice have low blood glucose levels [74]. Interestingly, crossing B6 dams and 129 sires normalized these severe phenotypes, suggesting that the cause lay in the recessive homozygous alleles in the B6 and 129 bkgds, and that these phenotypes, a consequence of the unnatural inbred strains, are not likely to represent human aniridia. To this point, of the seven epistatic interactions measured where one bkgd differed significantly from two non-significantly different bkgds, only one involved F1 mice as the variant. Therefore, in the development of new therapeutics for aniridia, where a phenotype that is caused by the *Pax6* mutation is desired, unobstructed by interaction with bkgd, we recommend using the genetically defined B6129F1 hybrid bkgd. As epistasis with inbred strains may confound the development of other therapeutics for other disorders too, the use of the defined hybrid B6129F1 mice, or indeed other hybrids, may broadly benefit the field.

Our results provide a description of epistasis between *Pax6* and three commonly used bkgds. The discovery of epistasis between *Pax6* genotype and B6 bkgd, presents a research opportunity to explore the factors that incline ocular development towards a moderate or severe phenotype in genetically identical eyes. Previous modifier studies for other genes have revealed that members of the same gene family can act as modifiers [75]. As other *PAX* transcription factors are involved in ocular development [76], we hypothesize that other *PAX* genes may be good initial candidates to modify the *Sey* phenotype.

Aniridia is often diagnosed after birth, when iris hypoplasia is easily observed [14, 77]. Therefore, important therapeutic timepoints for aniridia are the juvenile and adult eye. However, many descriptions of the *Sey* phenotype focus on the developing *Sey* eye and phenotypic descriptions of the adult *Pax6* haploinsufficiency mouse come from diverse sources that are spread across numerous *Pax6* mutations and bkgds [18, 22–24, 78]. In this context, our systematic evaluation of the Het phenotype, across three bkgds, bolsters the data available upon which evidence-based decisions can be made when evaluating new therapeutics for aniridia. We further think the B6129F1-*Sey* model may be useful in defining new human-relevant outcome measures for future therapeutics.

Acknowledgements The authors would like to acknowledge Dr. Michael S. Kobor for use of his Li-COR Odyssey system, Dr. Bjorn D. Bean for assistance in establishing our near-fluorescent western blotting protocol, Ms. Tess C. Lengyell and the Mouse Animal Production Service for providing mice for breeding and backcrossing, the CMMT Transgenic Facility for mouse husbandry support, Dr. Jingsong Wang and the British Columbia Children's Hospital Research Institute (BCCHRI) Imaging Core Facility for microscopy support, and Ms. Joanne Denny, Dr. Elizabeth Hui, and the BCCHRI Sequencing and Bioanalyzer Core for bioanalyzer support.

Funding This work was supported by an Aniridia Multi Investigator Grant from the Sharon Stewart Aniridia Research Trust [20R64586 to E.M.S.] and the Canadian Institutes of Health Research [MOP-119586 to E.M.S.]. Additionally, we acknowledge salary support from the University of British Columbia Four Year Doctoral Fellowship and Graduate Student Initiatives (to J.W.H.), and the Canadian Institutes of Health Research Canadian Graduate Scholarships (to J.W.H.).

Compliance with ethical standards

Conflict of interest The authors declare that they have no conflict of interest.

References

1. Yokoi T, Nishina S, Fukami M, Ogata T, Hosono K, Hotta Y, et al. Genotype-phenotype correlation of PAX6 gene mutations in aniridia. Hum Genome Var. 2016;3:15052.
2. Hingorani M, Williamson KA, Moore AT, van Heyningen V. Detailed ophthalmologic evaluation of 43 individuals with PAX6 mutations. Invest Ophthalmol Vis Sci. 2009;50:2581–90.
3. Ton CC, Hirvonen H, Miwa H, Weil MM, Monaghan P, Jordan T, et al. Positional cloning and characterization of a paired box- and homeobox-containing gene from the aniridia region. Cell. 1991;67:1059–74.
4. Jordan T, Hanson I, Zaletayev D, Hodgson S, Prosser J, Seawright A, et al. The human PAX6 gene is mutated in two patients with aniridia. Nat Genet. 1992;1:328–32.
5. Vincent MC, Pujo AL, Olivier D, Calvas P. Screening for PAX6 gene mutations is consistent with haploinsufficiency as the main mechanism leading to various ocular defects. Eur J Hum Genet. 2003;11:163–9.
6. Nelson LB, Spaeth GL, Nowinski TS, Margo CE, Jackson L. Aniridia. A review. Surv Ophthalmol. 1984;28:621–42.
7. Vasilyeva TA, Voskresenskaya AA, Kasmann-Kellner B, Khlebnikova OV, Pozdeyeva NA, Bayazutdinova GM, et al. Molecular analysis of patients with aniridia in Russian Federation broadens the spectrum of PAX6 mutations. Clin Genet. 2017;92:639–44.
8. Dubey SK, Mahalaxmi N, Vijayalakshmi P, Sundaresan P. Mutational analysis and genotype–phenotype correlations in southern Indian patients with sporadic and familial aniridia. Mol Vis. 2015;21:88–97.
9. Nishi M, Sasahara M, Shono T, Saika S, Yamamoto Y, Ohkawa K, et al. A case of novel de novo paired box gene 6 (PAX6) mutation with early-onset diabetes mellitus and aniridia. Diabet Med. 2005;22:641–4.
10. Yasuda T, Kajimoto Y, Fujitani Y, Watada H, Yamamoto S, Watarai T, et al. PAX6 mutation as a genetic factor common to aniridia and glucose intolerance. Diabetes. 2002;51:224–30.
11. Yogarajah M, Matarin M, Vollmar C, Thompson PJ, Duncan JS, Symms M, et al. PAX6, brain structure and function in human adults: advanced MRI in aniridia. Ann Clin Transl Neurol. 2016;3:314–30.
12. Grant MK, Bobilev AM, Pierce JE, DeWitte J, Lauderdale JD. Structural brain abnormalities in 12 persons with aniridia. F1000Research. 2017;6:255.
13. Sannan NS, Gregory-Evans CY, Lyons CJ, Lehman AM, Langlois S, Warner SJ, et al. Correlation of novel PAX6 gene abnormalities in aniridia and clinical presentation. Can J Ophthalmol. 2017;52:570–7.
14. Hingorani M, Hanson I, van Heyningen V. Aniridia. Eur J Hum Genet. 2012;10:1011–7.
15. Lee H, Khan R, O'Keefe M. Aniridia: current pathology and management. Acta Ophthalmol. 2008;86:708–15.
16. McClellan J, King MC. Genetic heterogeneity in human disease. Cell. 2010;141:210–7.
17. Rose AM, Shah AZ, Venturini G, Rivolta C, Rose GE, Bhattacharya SS. Dominant PRPF31 mutations are hypostatic to a recessive CNOT3 polymorphism in retinitis pigmentosa: a novel phenomenon of "linked trans-acting epistasis". Ann Hum Genet. 2014;78:62–71.
18. Ramaesh T, Collinson JM, Ramaesh K, Kaufman MH, West JD, Dhillon B. Corneal abnormalities in Pax6+/- small eye mice mimic human aniridia-related keratopathy. Invest Ophthalmol Vis Sci. 2003;44:1871–8.
19. Lim HT, Kim DH, Kim H. PAX6 aniridia syndrome: clinics, genetics, and therapeutics. Curr Opin Ophthalmol. 2017;5:436–47.
20. Hogan BL, Hirst EM, Horsburgh G, Hetherington CM. Small eye (Sey): a mouse model for the genetic analysis of craniofacial abnormalities. Development . 1988;103:115–9.
21. Clayton RM, Campbell JC. Small eye, a mutant in the house mouse apparently affecting the synthesis of extracellular membranes. J Physiol. 1968;198:74–5.
22. Li S, Goldowitz D, Swanson DJ. The requirement of pax6 for postnatal eye development: evidence from experimental mouse chimeras. Invest Ophthalmol Vis Sci. 2007;48:3292–300.
23. Gregory-Evans CY, Wang X, Wasan KM, Zhao J, Metcalfe AL, Gregory-Evans K. Postnatal manipulation of Pax6 dosage reverses congenital tissue malformation defects. J Clin Invest. 2013;124:111–6.
24. Wang X, Gregory-Evans K, Wasan KM, Sivak O, Shan X, Gregory-Evans CY. Efficacy of postnatal in vivo nonsense suppression therapy in a Pax6 mouse model of aniridia. Mol Ther Nucleic Acids. 2017;7:417–28.
25. Hill RE, Favor J, Hogan BL, Ton CC, Saunders GF, Hanson IM, et al. Mouse small eye results from mutations in a paired-like homeobox-containing gene. Nature. 1991;354:522–5.
26. Roberts RC. Small-eyes, a new dominant mutant in the mouse. Genet Res. 1967;9:121–2.
27. van Heyningen V, Williamson KA. PAX6 in sensory development. Hum Mol Genet. 2002;11:1161–7.
28. Tzoulaki I, White IM, Hanson IM. PAX6 mutations: genotype–phenotype correlations. BMC Genet. 2005;6:27.
29. Gregory-Evans K, Cheong-Leen R, George SM, Xie J, Moosajee M, Colapinto P, et al. Non-invasive anterior segment and posterior segment optical coherence tomography and phenotypic characterization of aniridia. Can J Ophthalmol. 2011;46:337–44.
30. Kanakubo S, Nomura T, Yamamura K-i, Miyazaki J-i, Tamai M, Osumi N. Abnormal migration and distriubution of neural crest cells in *Pax6* heterozygous mutant eye, a model for human eye diseases. Genes Cells. 2006;11:919–33.
31. Gronskov K, Olsen JH, Sand A, Pedersen W, Carlsen N, Bak Jylling AM, et al. Population-based risk estimates of Wilms tumor in sporadic aniridia. A comprehensive mutation screening procedure of PAX6 identifies 80% of mutations in aniridia. Hum Genet. 2001;109:11–8.
32. Favor J, Peters H, Hermann T, Schmahl W, Chatterjee B, Neuhauser-Klaus A, et al. Molecular characterization of Pax6(2Neu) through Pax6(10Neu): an extension of the Pax6 allelic series and the identification of two possible hypomorph alleles in the mouse Mus musculus. Genetics. 2001;159:1689–700.
33. Keane TM, Goodstadt L, Danecek P, White MA, Wong K, Yalcin B, et al. Mouse genomic variation and its effect on phenotypes and gene regulation. Nature. 2011;477:289–94.

34. Silva AJ, Simpson EM, Takahashi JS, Lipp H-P, Nakanishi S, Wehner JM, et al. Mutant mice and neuroscience: recommendations concerning genetic background. Neuron. 1997;19:755–9.
35. Zuberi A, Lutz C. Mouse models for drug discovery. Can new tools and technology improve translational power? Ilar J. 2016;57:178–85.
36. Dora NJ, Collinson JM, Hill RE, West JD. Hemizygous Le–Cre transgenic mice have severe eye abnormalities on some genetic backgrounds in the absence of LoxP sites. PLoS ONE. 2014;9: e109193.
37. Sorge RE, Martin LJ, Isbester KA, Sotocinal SG, Rosen S, Tuttle AH, et al. Olfactory exposure to males, including men, causes stress and related analgesia in rodents. Nat Methods. 2014;11:629–32.
38. Hummel KP, Coleman DL, Lane PW. The influence of genetic background on expression of mutations at the diabetes locus in the mouse. I. C57BL-KsJ and C57BL-6J strains. Biochem Genet. 1972;7:1–13.
39. Favor J, Bradley A, Conte N, Janik D, Pretsch W, Reitmeir P, et al. Analysis of Pax6 contiguous gene deletions in the mouse, Mus musculus, identifies regions distinct from Pax6 responsible for extreme small-eye and belly-spotting phenotypes. Genetics. 2009;182:1077–88.
40. Fontaine DA, Davis DB. Attention to background strain is essential for metabolic research: C57BL/6 and the international knockout mouse consortium. Diabetes. 2016;65:25–33.
41. Mishina M, Sakimura K. Conditional gene targeting on the pure C57BL/6 genetic background. Neurosci Res. 2007;58:105–12.
42. Seong E, Saunders TL, Stewart CL, Burmeister M. To knockout in 129 or in C57BL/6: that is the question. Trends Genet. 2004;20:59–62.
43. Kanakubo S, Nomura T, Yamamura KI, Miyazaki JI, Tamai M, Osumi N. Abnormal migration and distribution of neural crest cells in Pax6 heterozygous mutant eye, a model for human eye diseases. Genes Cells. 2006;11:919–33.
44. Wang X, Shan X, Gregory-Evans CY. A mouse model of aniridia reveals the in vivo downstream targets of Pax6 driving iris and ciliary body development in the eye. Biochim Biophys Acta. 2016;1863:60–7.
45. Schedl A, Ross A, Lee M, Engelkamp D, Rashbass P, van Heyningen V, et al. Influence of PAX6 gene dosage on development: overexpression causes severe eye abnormalities. Cell. 1996;86:71–82.
46. Duan D, Fu Y, Paxinos G, Watson C. Spatiotemporal expression patterns of Pax6 in the brain of embryonic, newborn, and adult mice. Brain Struct Funct. 2013;218:353–72.
47. Leo S, Straetemans R, D'Hooge R, Meert T. Differences in nociceptive behavioral performance between C57BL/6J, 129S6/SvEv, B6 129 F1 and NMRI mice. Behav Brain Res. 2008;190:233–42.
48. Graves L, Dalvi A, Lucki I, Blendy JA, Abel T. Behavioral analysis of CREB alphadelta mutation on a B6/129 F1 hybrid background. Hippocampus. 2002;12:18–26.
49. Hickmott JW, Chen CY, Arenillas DJ, Korecki AJ, Lam SL, Molday LL, et al. PAX6 MiniPromoters drive restricted expression from rAAV in the adult mouse retina. Mol Ther Methods Clin Dev. 2016;3:16051.
50. de Leeuw CN, Korecki AJ, Berry GE, Hickmott JW, Lam SL, Lengyell TC, et al. rAAV-compatible MiniPromoters for restricted expression in the brain and eye. Mol Brain. 2016;9:52.
51. Bui M, Liu Z. Simple allele-discriminating PCR for cost-effective and rapid genotyping and mapping. Plant Methods. 2009;5:1.
52. Vandesompele J, De Preter K, Pattyn F, Poppe B, Van Roy N, De Paepe A, et al. Accurate normalization of real-time quantitative RT-PCR data by geometric averaging of multiple internal control genes. Genome Biol. 2002;3:Research0034.1–research.11.
53. Ouyang H, Xue Y, Lin Y, Zhang X, Xi L, Patel S, et al. WNT7A and PAX6 define corneal epithelium homeostasis and pathogenesis. Nature. 2014;511:358–61.
54. Keppel G, Wickens TD. Design and analysis: a researcher's handbook. 4th ed. (Pearson Prentice Hall, Upper Saddle River, N. J., 2004).
55. Lykke-Andersen S, Jensen TH. Nonsense-mediated mRNA decay: an intricate machinery that shapes transcriptomes. Nat Rev Mol Cell Biol. 2015;16:665–77.
56. Latta L, Viestenz A, Stachon T, Colanesi S, Szentmáry N, Seitz B, et al. Human aniridia limbal epithelial cells lack expression of keratins K3 and K12. Exp eye Res. 2017;167:100–9.
57. Liu Q, Wan W, Liu Y, Liu Y, Hu Z, Guo H, et al. A novel PAX6 deletion in a Chinese family with congenital aniridia. Gene. 2015;563:41–4.
58. Zhang R, Linpeng S, Wei X, Li H, Huang Y, Guo J, et al. Novel variants in PAX6 gene caused congenital aniridia in two Chinese families. Eye. 2017;31:956–61.
59. Graw J, Loster J, Puk O, Munster D, Haubst N, Soewarto D, et al. Three novel Pax6 alleles in the mouse leading to the same small-eye phenotype caused by different consequences at target promoters. Invest Ophthalmol Vis Sci. 2005;46:4671–83.
60. Rossi A, Kontarakis Z, Gerri C, Nolte H, Holper S, Kruger M, et al. Genetic compensation induced by deleterious mutations but not gene knockdowns. Nature. 2015;524:230–3.
61. De Souza AT, Dai X, Spencer AG, Reppen T, Menzie A, Roesch PL, et al. Transcriptional and phenotypic comparisons of Ppara knockout and siRNA knockdown mice. Nucleic Acids Res. 2006;34:4486–94.
62. El-Brolosy MA, Stainier DYR. Genetic compensation: a phenomenon in search of mechanisms. PLoS Genet. 2017;13:e1006780.
63. Grindley JC, Davidson DR, Hill RE. The role of Pax-6 in eye and nasal development. Development. 1995;121:1433–42.
64. Mastick GS, Davis NM, Andrew GL, Easter SS Jr.. Pax-6 functions in boundary formation and axon guidance in the embryonic mouse forebrain. Development . 1997;124:1985–97.
65. Lou CH, Shao A, Shum EY, Espinoza JL, Huang L, Karam R, et al. Posttranscriptional control of the stem cell and neurogenic programs by the nonsense-mediated RNA decay pathway. Cell Rep. 2014;6:748–64.
66. Bruno IG, Karam R, Huang L, Bhardwaj A, Lou CH, Shum EY, et al. Identification of a microRNA that activates gene expression by repressing nonsense-mediated RNA decay. Mol Cell. 2011;42:500–10.
67. Aota S, Nakajima N, Sakamoto R, Watanabe S, Ibaraki N, Okazaki K. Pax6 autoregulation mediated by direct interaction of Pax6 protein with the head surface ectoderm-specific enhancer of the mouse Pax6 gene. Dev Biol. 2003;257:1–13.
68. Xiao X, Li S, Zhang Q. Microphthalmia, late onset keratitis, and iris coloboma/aniridia in a family with a novel PAX6 mutation. Ophthalmic Genet. 2012;33:119–21.
69. Deml B, Reis LM, Lemyre E, Clark RD, Kariminejad A, Semina EV. Novel mutations in PAX6, OTX2 and NDP in anophthalmia, microphthalmia and coloboma. Eur J Hum Genet. 2016;24:535–41.
70. Williamson KA, FitzPatrick DR. The genetic architecture of microphthalmia, anophthalmia and coloboma. Eur J Med Genet. 2014;57:369–80.
71. Henderson RA, Williamson K, Cumming S, Clarke MP, Lynch SA, Hanson IM, et al. Inherited PAX6, NF1 and OTX2 mutations in a child with microphthalmia and aniridia. Eur J Hum Genet. 2007;15:898–901.
72. Mauri L, Franzoni A, Scarcello M, Sala S, Garavelli L, Modugno A, et al. SOX2, OTX2 and PAX6 analysis in subjects with anophthalmia and microphthalmia. Eur J Med Genet. 2015; 58:66–70.

73. Chase HB. Studies on an anophthalmic strain of mice. III. Results of crosses with other strains. Genetics. 1942;27:339–48.
74. Kulkarni RN, Almind K, Goren HJ, Winnay JN, Ueki K, Okada T, et al. Impact of genetic background on development of hyperinsulinemia and diabetes in insulin receptor/insulin receptor substrate-1 double heterozygous mice. Diabetes. 2003;52:1528–34.
75. Houde C, Banks KG, Coulombe N, Rasper D, Grimm E, Roy S, et al. Caspase-7 expanded function and intrinsic expression levels underlies strain-specific brain phenotype of caspase-3-null mice. J Neurosci. 2004;24:9977–84.
76. Kozmik Z. Pax genes in eye development and evolution. Curr Opin Genet Dev. 2005;15:430–8.
77. Richardson R, Hingorani M, Van Heyningen V, Gregory-Evans C, Moosajee M. Clinical utility gene card for: aniridia. Eur J Hum Genet. 2016;24:e1–e4.
78. Hart AW, Mella S, Mendrychowski J, van Heyningen V, Kleinjan DA. The developmental regulator Pax6 is essential for maintenance of islet cell function in the adult mouse pancreas. PLoS ONE. 2013;8:e54173.